IEEE Internet of Things Journal, Volume 9, Number 12, 15 June 2022, pp. 9831-9842
DOI:10.1109/JIOT.2022.3153637

Error Performance and Mutual Information for IoNT Interface System

Yu Li, Lin Lin, Weisi Guo, Dingguo Zhang, and Kun Yang

***Abstract*—Molecular communication and the internet of nanothings (IoNTs) are emerging research hotspots recently, which show great potential in biomedical applications inside the human body. However, how to transmit information from inside body IoNTs to outside devices is seldomly studied. It is well known that the nervous system is responsible for perceiving the external environment and controlling the feedback signals. It exactly works like an interface between the external and internal environment. Inspired by this, this paper proposes a novel concept that one can use the modified nervous system to communicate between IoNT devices and in vitro equipments. In our proposed system, nanomachines transmit signals via stimulating the nerve fiber by the electrode. Then the signals transmit along nerve fibers and muscle fibers. Finally, they cause changes in surface electromyography (sEMG) signals which can be decoded by the body surface receiver. The paper presents the framework of this entire through-body communication system. Each part of the framework is also mathematically modeled. The error probability and mutual information of the system are derived from the communication theory perspective, which are evaluated and analyzed through numerical results. This study can pave the way for the connection of IoNT in vivo to external networks.**

***Index Terms*—Internet of nanothings, interface, molecular communication, error performance, mutual information.**

I. Introduction

WITH the development of nanotechnology and biology, the implementation of nanodevices becomes possible [2]. Nanodevices can only perform basic tasks such as sensing, actuation, and storage due to volume limitation. Whereas through the communication and cooperation between nanomachines, the nanonetworks can realize more advanced biomedical applications such as targeted drug delivery and disease treatment [3], [4]. Due to high bio-compatibility and low power consumption, molecular communication (MC) becomes the most potential communication paradigm for nanonetworks and has been studied intensively in recent years [5]–[8].

Actually, in many applications nanomachines also need to communicate with devices in other networks. For instance, in MC, a group of envisioned nanomachines cooperate to implement some complex tasks such as targeted drug delivery, early disease diagnosis, and health monitoring, so in vivo nanomachines need to communicate with devices outside the body. However, most of the current work on MC and IoNTs is within a limited range such as the in-vivo environment. It is still a challenge that implement an interface to transfer information from implanted IoNT devices to external devices. Since these nano-scale devices can not communicate directly with electromagnetic wave based devices, it is necessary to build such an interface. It allows the monitoring signals and control signals to be shared between inside body devices and outside body processing center. This research issue may be the first step of making IoNT applications possible. It is an important issue that future IoNT applications rely on, and it is the supporting technology of IoNT [9].

In the literature, there are not many preliminary investigations. In [10], the authors fix a probe in blood vessels as an interface for information exchange. The working environment of IoNT devices is exactly the blood circulation system in the human body. It is assumed that the probe can transmit signals to the outside world by inducing allergic reactions on the skin surface or emitting infrared or ultrasonic waves. However, the authors only propose a conjecture and do not give a detailed method to implement it.

Another interface is proposed in [11], which is an interactive display below the skin that can realize the mutual conversion between fluorescent signals and biochemical signals. It consists of several bionanomachines which can convert the external mechanical pressure into biochemical signals. The in vivo nanomachines can recognize those biochemical particles. This interface can also realize the signal transmission from inside to outside body through the fluorescence of the display, which may need highly complex external detection devices.

In [12], an interface based on magnetic nano-particles is proposed. It is assumed that nanomachines can release magnetic particles when they detect signal molecules. These magnetic nanoparticles transmit signals to external devices by moving and changing the current in the external coil. But this scheme has a key problem reusing the magnetic particles because of the loading capacity of nanomachines. They cannot emit magnetic particles indefinitely. In addition, it is also necessary

This work was supported in part by National Natural Science Foundation, China (61971314), in part by Science and Technology Commission of Shanghai Municipality (19510744900), in part by Sino-German Center of Intelligent Systems, Tongji University, in part by the Fundamental Research Funds for the Central Universities (Grant No. ZYGX2019J001), and in part by UESTC Yangtze Delta Region Research Institute - Quzhou (Grant No.: 2021D003). Part of this work was presented at the IEEE GLOBECOM 2020 [1]. (*Corresponding author: Lin Lin.*)

Y. Li and L. Lin are with the College of Electronics and Information Engineering, Tongji University, Shanghai, 201804, China (e-mail: 1930703@tongji.edu.cn; fxlinlin@tongji.edu.cn).

W. Guo is with the Centre for Autonomous and Cyberphysical Systems, Cranfield University, Milton Keynes, MK43 0AL, UK (e-mail: weisi.guo@cranfield.ac.uk).

D. Zhang is with the Department of Electronic and Electrical Engineering, University of Bath, Bath, BA2 7AY, UK (e-mail: d.zhang@bath.ac.uk).

K. Yang is with the Yangtze Delta Region Institute, University of Electronic Science and Technology of China, Quzhou, 324000, China, and also with the School of Computer Science and Electronic Engineering, University of Essex, Colchester, CO4 3SQ, UK (e-mail: kunyang@essex.ac.uk).

to consider that magnetic materials may have a negative impact on the biological environment. There are also some other proposals for instance using sweat to transmit signals [13] and taking the advantage of quorum sensing mechanisms of bacteria [14], such as synthesizing the fluorescent protein.

Until now, designing a suitable interface between the nanoscale environment and the external macro world is still an open research issue. However, we have noticed that there is already a good paradigm in nature to solve this problem. That is the nervous system. People can interact with the external environment with the help of nervous system, which contains three functions: sensory input, information integration, and motor output [15]. The corresponding interaction process includes: perceiving stimuli, information processing, and responding.

In the literature, there are plenty of theoretical and experimental evidence which can support the proposal of using neural pathways to transmit information. In [16], a channel model of neuro-spike communication at nanoscale is proposed and the method of extending it into a multi-terminal nervous system nanonetwork is also discussed. In [17], the maximum achievable transmission range and the maximum sustainable bit rate of action potential (AP) along the nerve are determined. Besides, two ICT-based treatment approaches for spinal cord injuries are introduced in [18]. In [19], the authors present experimental evidence for controlled information transfer through in vivo nervous system. Moreover, neurostimulation technique is used to treat disease [20]. A novel neural stimulator is presented in [21].

Inspired by the evidence, this paper proposes that one can use the modified neural system as a data transmission interface to transmit signals between internal IoNTs and external devices. The main contributions of this paper are:

1) We propose a novel interface system which can transmit signals between in-vivo applications and external environment and present the framework of the entire interface system.

2) We mathematically model every part of the proposed framework.

3) The error probability and mutual information (MI) of the entire interface system are evaluated and discussed from the communication perspective.

The remainder of the paper is organized as follows. In Section II the preliminary knowledge of neurons and nervous system is introduced. In Section III the framework is presented and Section IV gives the mathematical model of the proposed interface system. The possible construction strategy of the system framework is discussed in Section V. Mutual information of the proposed framework is derived in Section VI. Then Section VII presents the simulation results of our proposed system such as error performance and mutual information. Finally, Section VIII summarizes the main contents.

II. Preliminaries

The human nervous system contains two main parts: the central and peripheral nervous systems. The central nervous system is the main control center of the human body which includes the brain and spinal cord. Whereas the peripheral system, which is composed of all the nerves that branch off from the brain and spine, provides a bridge between the central nervous system and the execution system. The peripheral system can transmit signals in two directions. The sensory division transmits sensory stimuli in the direction towards the brain and spinal cord. The motor division, on the contrary, sends commands from the central nervous system to the muscles and glands. In order to avoid affecting important physiological activities, our system is based on the somatic nervous system, which is a part of the motor division and controls the movement of the skeletal muscle.

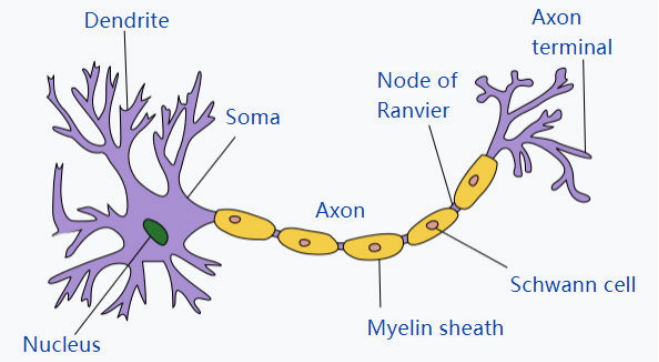

Fig. 1. The basic composition of a neuron [22].

The nervous system is mainly composed of neurons. To make better use of neural pathways, we need to understand the mechanism of neural communication first of all. As shown in Fig. 1, a neuron is composed of three main parts: 1) *Dendrites*. They receive signals from the previous neuron and transmit them to the soma. 2) *Soma*. It is also called cell body which contains many organelles and the nucleus. 3) *Axon*. It is the transmission channel of AP. Axon usually has multiple branches at the end and each end of the branch can expand to form a synapse. Axon is exactly the structure that conveys signals to the next neuron. Whereas the synapse is the structure that converts the electrical signal into a chemical signal.

Neural communication is implemented by mutual conversion of electrical and chemical signals. But only electrical impulse can be transmitted on a single neuron whose strength and speed are usually constant [23]. The whole process of neuron generation AP is described in Fig. 2:

1) The initial state is the resting state in which sodium-potassium pumps, potassium channels, and sodium channels are all closed. Since the positive ions outside the membrane is much more than inside the membrane, it is negatively charged inside the cell. The voltage difference between the two sides of the membrane is called resting membrane potential, which is about $-70\,\text{mV}$ [24].

2) Next state is depolarization. When the membrane potential reaches over the threshold $-55\,\text{mV}$ under the action of the stimulus, the sodium channels will open (Fig. 2-2). They allow sodium ions to come into the cell by passing through the cell membrane. Then the intracellular negative charge can be neutralized, which results in a net positive intracellular charge. The maximum membrane potential can reach $40\,\text{mV}$.

3) The state in Fig. 2-3 is repolarization. After the peak

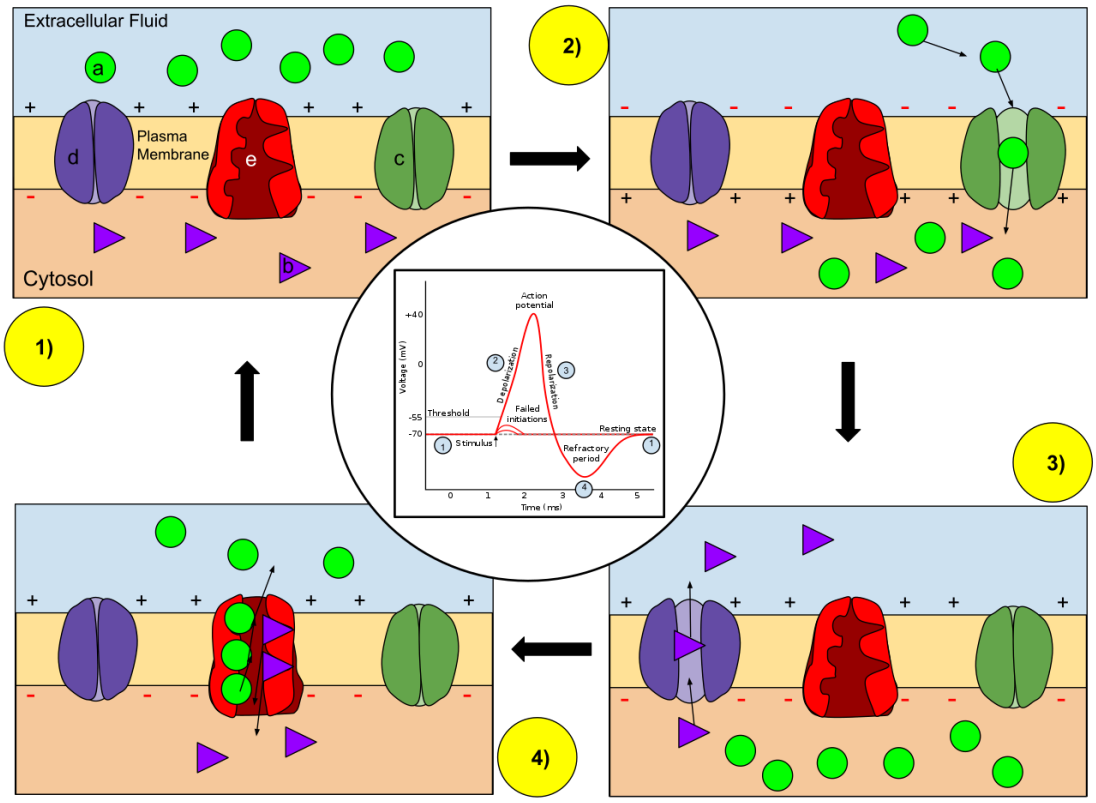

Fig. 2. The process by which neuron membrane generates APs. Here, a represents sodium (Na^+) ion, b denotes potassium (K^+) ion, c denotes voltage-gated sodium channel, d is voltage-gated potassium channel, and e represents sodium-potassium pump. (1) The membrane is in resting state. Now ungated ion channels work to make the ionic current flow into and out of the cell membrane in equilibrium. (2) The membrane is in depolarization state. Under the action of the stimulus, the voltage-gated sodium ion channel opens. As sodium ions flow into the cell, the membrane potential changes from negative potential to positive potential. (3) The membrane is in repolarization state. After the membrane potential reaches its peak, voltage-gated sodium channels are closed, whereas voltage-gated potassium channels open. With the outflow of potassium ions, the membrane potential returns to negative. (4) The membrane is in refractory state. At this time, voltage-gated channels no longer or are difficult to respond to the depolarizing stimulus. Besides, the membrane potential slowly returns to resting state as sodium-potassium pumps continuously pump in sodium ions and pump out potassium ions against the concentration gradient [22].

membrane potential, the sodium channels close and potassium channels open, allowing potassium ions to flow into the extracellular fluid. Then the membrane potential gradually decreases until it is below $-70\,\mathrm{mV}$ and the hyperpolarization process starts when the voltage will continue to drop to about $-90\,\mathrm{mV}$.

4) The last state is refractory period. The sodium-potassium pump opens in this period, allowing Na^+ and K^+ ions to return to their resting state distributions inside and outside the membrane.

Since there are lots of voltage-gated sodium channels on axons, local currents can trigger adjacent channels. Therefore, APs are conveyed to the end of the axon. When the AP gets to synapses, the vesicles stored here will fuse with presynaptic membrane and release neurotransmitters. These neurotransmitters will bind to receptors on the postsynaptic neuron after they diffuse through the synaptic cleft. Through the above process, two neurons can complete the transmission of information.

Next, we propose the framework of our IoNT interface system based on the existing nervous system in human body.

III. Proposed System Framework

In this section, we introduce the framework of our proposed interface system and illustrate the whole communication process between the in vivo IoNT devices and the outside-body processing unit. Firstly an interface between nanomachines and nervous system should be established. As a result, in vivo IoNTs can upload data to the nerve fiber and transmit it outside the body through muscle contraction. The extracorporeal device detects muscle contraction by monitoring and analyzing surface electromyography (sEMG), thereby decoding the information transmitted from implanted IoNTs inside the body.

The entire proposed framework is shown in Fig. 3-a. Assume the IoNT devices are implanted in blood vessels. These nanomachines communicate with the base station (BS) by MC in a single-hop or multi-hop manner. The BS is exactly the only interface between the IoNT and nervous system. It is responsible for integrating data from nanomachines in IoNT and converting the data into nerve fiber stimuli in order to transmit signals outside the body.

BS is deployed as close as possible to the nerves that need to transmit signals and fixed on the inner wall of the blood vessel. Consider the BS is connected to a tiny wire with an electrode to stimulate the nerve fiber. The electrode is directly

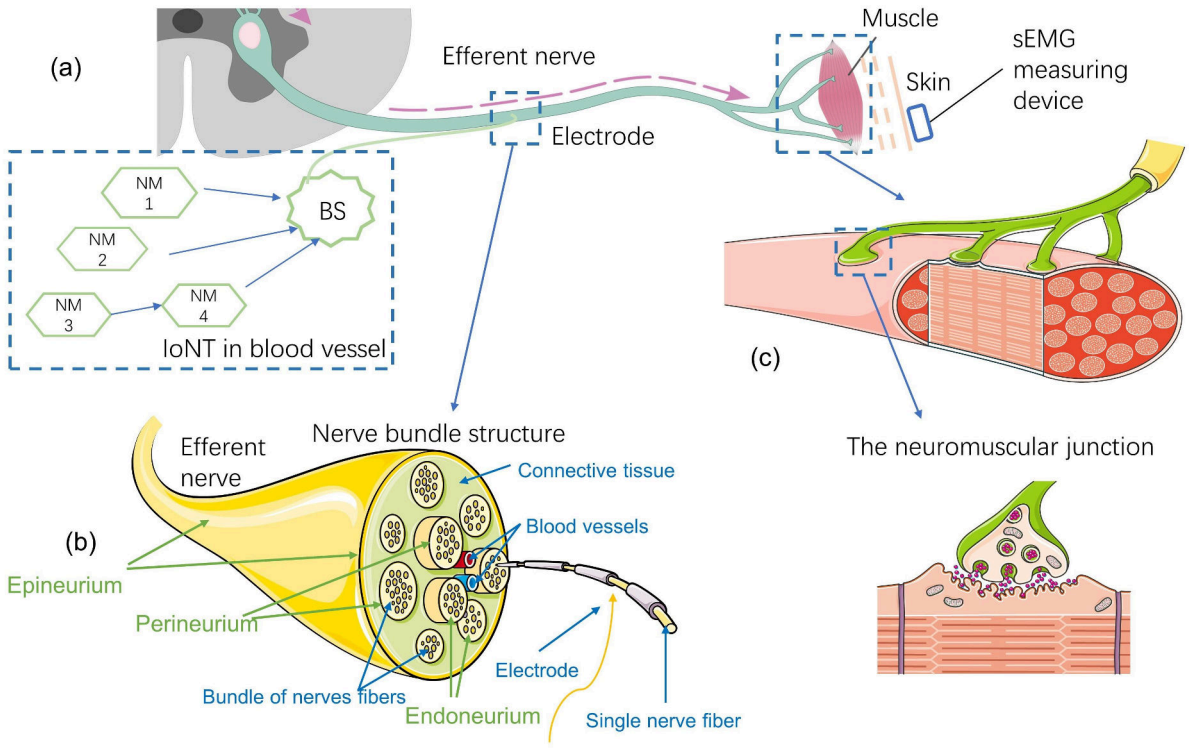

Fig. 3. The framework of our proposed system. In this interface system, we only consider the transfer of data from nanomachines of in-body IoNT to devices outside the body. a) The entire composition of the proposed interface framework. The left dotted box denotes implanted IoNT devices in blood vessel. The BS which connects an electrode, is in charge of collecting data sent from the IoNT and encoding information into a stimulating current. The stimuli sent by the BS can generate APs on the axon. They are transmitted to the synapse via the axon, causing neurotransmitter release and finally triggering the excitement of postsynaptic muscle cells. Extracorporeal equipment can detect changes in surface electromyography caused by muscle contraction to decode the signals transmitted from the in-body IoNT. b) Illustration of the structure of nerve bundles in the peripheral nervous system. The peripheral nerve bundle which looks like a cable, generally includes three layers of membranes, which are insulating connective tissue that surround axons and blood vessels and separate them from each other. In addition, these layers can protect and support nerve fibers. c) Illustration of the motor endplate. Motor endplate, also called the neuromuscular junction, is composed of the end terminal of motor neuron axon and the muscle fiber. It is an effector that can control muscle contraction. There are several unmyelinated branches at the end of the axon extending to the skeletal muscle to form motor endplates. At the bottom of the figure, an enlarged view of the neuromuscular junction is shown.

connected to the nerve fiber. In [25], [26], similar devices are mentioned. In order to avoid affecting important physiological activities of the nervous system, the nerves used to transmit signals should be skeletal muscle nerves that are not frequently used. And because the efferent nerve only transmits signals in one direction, the stimulus signals are not transmitted to the central nervous system such as the brain and spinal cord.

Fig. 3-b represents the membrane structures of nerve bundles in the peripheral nervous system. Understanding the composition of nerve bundles helps us to deploy stimulation electrodes. In a nerve bundle, nerve fibers and blood vessels are separated and supported by three layers of insulating connective tissue membranes, which are endoneurium, perineurium and epineurium. The endoneurium is the inner layer surrounding myelin sheath of the axon. The perineurium is the insulating membrane that forms the membrane of nerve fascicles which contain several axons. It can selectively allow substances to enter or leave nerve fibers. The epineurium is the outermost layer of nerve bundles. It surrounds several nerve fascicles [27] which finally form a complete nerve bundle. In this paper, it is assumed that the electrode is implanted in the nerve fascicle and can selectively stimulate one axon.

We have mentioned earlier that the BS collects data from the IoNT and encodes the information into stimulus current. This electric current is delivered to the electrode and induces axons to generate APs. Next, the AP travels to the neuromuscular junction (NMJ) and causes neurotransmitters to be released from the synapse. These neurotransmitters can bind to receptors on the postsynaptic muscle cell membrane, so the muscle fiber contracts which results in changes in the surface electromyographic (sEMG). Considering that there is an external device that is attached to the skin surface, it can detect sEMG easily or at least detect changes in sEMG.

In the following section, the proposed framework is mathematically modeled.

IV. Mathematical Model of Proposed Framework

This section presents the mathematical model of our proposed interface system.

The main signals flow in this interface system are defined as: bits sent from in vivo IoNT devices which are collected by the BS $x \in \{0, 1\}$, the stimulating current which is encoded

TABLE I
TYPICAL VALUES FOR MODEL PARAMETERS

Parameter	Value
resistivity of extracellular matrix ρ_e	300 Ω·cm [28]
neuron resting potential V_r	-80 mV [29]
axon diameter d_a	20 μm [28]
membrane capacitance c_m	2 μF/cm^2 [28]
nodal gap width l	2.5 μm [28]
length between two nodes L	2 mm [28]
axoplasm resistivity ρ_i	110 Ω·cm [28]
conductance for sodium g_{Na}	1445 kΩ^{-1}cm^{-2} [29]
maximum conductance for leakage currents g_L	128 kΩ^{-1}cm^{-2} [29]
equilibrium membrane potentials for sodium V_{Na}	115 mV [29]
equilibrium membrane potentials for leakage ions V_L	-0.01 mV [29]
neural action potential threshold V_h	-55 mV
muscle fibers' action potential threshold V_{mth}	-50 mV [30]
diameter of the muscle fiber d_m	25 μm [31]
conductivity of the intracellular axoplasm σ_a	1.01 mho/m [31]
muscle fiber conduction velocity v	5 m/s [32]
radial conductivity of the external medium σ_r	0.063 mho/m [32]
axial extracellular conductivity σ_z	0.33 mho/m [32]

by the BS and sent to the electrode $A(t)$, extra-membrane potential after stimulation V_0, membrane potential at the nth node of Ranvier V_n, the total number of neurotransmitters released at one time Q, amount of neurotransmitters that bind to receptors on the postsynaptic muscle membrane Q_a, the endplate membrane potential caused by the combination of neurotransmitters V_{ep}, AP transmitted on the muscle fiber V_{mu}, sEMG signal V_s, and decoded bits at the receiver $\hat{x}$. In the following, the mathematical relationships of these signals are introduced. Some typical values in the literature for model parameters are summarized and shown in Table I.

In this paper, we apply OOK modulation scheme at the BS. The stimulating current sent by the BS is defined as

$$A(t) = \begin{cases} I, & x = 1 \\ 0, & x = 0, \end{cases} \tag{1}$$

where $A(t)$ denotes the electric current, and I is the stimulus signal when bit "1" needs to be transmitted from the BS. Here the stimulation current I can be any microcurrent that is physiologically reasonable and can induce action potentials, such as currents of micro stimulators in medical applications that require selective stimulation of nerves [33].

Next, the electric current $A(t)$ is delivered to neuron axon by a point electrode. Here we ignore the effects caused by non-linear factors such as the impact caused by connective tissue and the anisotropy of nerve fibers. So the extra-membrane potential V_0 is defined as [28]

$$V_0 = \frac{\rho_e I}{4\pi d_e}, \tag{2}$$

where I is the stimulation current in (1), ρ_e is resistivity of extracellular matrix, d_e is the distance between the membrane and the electrode. Since the nerve fiber in our system is myelinated, we adopt the myelinated cable equation proposed by McNeal. The membrane potential at the nth node of Ranvier (gap between two myelin-sheaths), denoted as V_n, is formulated as

$$V_n = V_{i,n} - V_{e,n} - V_r, \tag{3}$$

where $V_{i,n}$ is the intracellular potential at node n, $V_{e,n}$ is the extracellular potential. V_r denotes the resting potential of this neuron axon, which is usually -80 mV [29]. Besides, the variation of membrane potential $\frac{dV_n}{dt}$, can be defined as [28]

$$\begin{aligned} \frac{dV_n}{dt} =& \frac{1}{c_m}[\frac{d_a}{4\rho_i}(\frac{V_{n-1} - 2V_n + V_{n+1}}{lL} + \\ & \frac{V_{e,n-1} - 2V_{e,n} + V_{e,n+1}}{lL} - i_{ion,n})], \end{aligned} \tag{4}$$

where d_a is the diameter of the axon in the myelin sheath, c_m is membrane capacitance per unit area, l is the width of nodal gap, n is the sequence number of the node, L is the length between two nodes, which is proportional to axon diameter, ρ_i is axoplasm resistivity, $i_{ion,n}$ is the ionic current at the nth segment according to CRRSS model mentioned in [29]. Typical parameter values for relevant models in the literature are given in Table I.

When the AP is transmitted from the last node n to the synapse at the end of the axon, synaptic vesicles in the presynapse may fuse with presynaptic membrane and release neurotransmitters into the synaptic cleft. Define this fusion probability as p_r and the amount of neurotransmitters released into synaptic cleft as Q'. If this number is influenced by the membrane potential V_n at node n, it is presented as

$$Q' = f_s(V_n) = \begin{cases} Q, & V_n \geq V_h \\ 0, & V_n < V_h, \end{cases} \tag{5}$$

where $f_s(x)$ denotes the relationship between Q' and V_n. Neurotransmitters will be released when V_n is larger than the action potential threshold V_h, which is approximately -55 mV. So $f_s(\cdot)$ can be regarded as a decision function. Further, it is assumed that the amount of neurotransmitters in each vesicle is the same, which is based on experimental observations and hypotheses in [34], [35]. The number of neurotransmitters is represented as N_n. There are n_v vesicles in readily releasable vesicle pool. According to the central limit theorem, the expectation of the amount Q of neurotransmitters actually released follows Gaussian distribution. We have

$$EQ \sim N(\mu, \sigma^2), \tag{6}$$

where μ and σ^2 are expressed respectively as

$$\begin{aligned} \mu =& p_r N_n n_v, \\ \sigma^2 =& p_r(1 - p_r) N_n n_v. \end{aligned} \tag{7}$$

The released neurotransmitters diffuse across the synapse cleft and finally bind to receptors in muscle membrane. We define the binding amount of neurotransmitters as Q_a, which is a random variable. Here we adopt a model about hitting probability of the neurotransmitter mentioned in [36] which is defined as

$$F(t) = \frac{r}{d + r} erfc(\frac{d}{\sqrt{4Dt}}), \tag{8}$$

where t is the time, r is the receiving radius of the postsynaptic membrane which is regarded as a receiver, d is the distance of

synaptic cleft, D denotes the diffusion coefficient of synaptic cleft medium, $erfc(\cdot)$ denotes the complementary error function. Although there are more accurate models specifically for synaptic channels in the literature [37], [38], in order to facilitate modeling, we chose not to consider the geometry of the synaptic channel, and only model the basic communication process of the neuromuscular junction.

In this model, it is assumed that whether a single neurotransmitter binds to the postsynaptic membrane receptor follows the binomial distribution of the parameter $F(t)$. Since Q is usually greater than 100, it can be considered that Q_a obeys a Gaussian distribution, and its mean and variance are denoted as $Q \cdot F(t)$ and $Q \cdot F(t)(1-F(t))$ respectively [39]. Here we only focus on a single symbol. In fact, the symbol sequence previously transmitted will also affect Q_a. In the next section we will consider inter-symbol interference (ISI) for the symbol sequence to calculate mutual information.

The binding of neurotransmitters to receptors on the postsynaptic muscle membrane will cause changes in muscle membrane potential. This membrane potential is called endplate membrane potential V_{ep}, which is defined as

$$V_{ep} = f_m(Q_a). \tag{9}$$

During the depolarization process before the action potential is generated, we simplify the relationship $f_m(\cdot)$ to a linear relationship [34], [35]. This is because the postsynaptic membrane is depolarized in a graded manner [34]. The size of the blip is fixed due to the fixed size of the quantum (vesicle), which means the underlying assumption that the impact of each neurotransmitter had on the postsynaptic membrane potential is the same. So it is reasonable that the postsynaptic membrane potential is assumed proportional to the number of neurotransmitters bound to it if action potentials are not considered.

V_{ep} is the decisive factor affecting the on-off state of voltage-gated ion channels. These ion channels can cause changes in the membrane potential of muscle fiber to generate muscle APs V_{mu}, which is the same as the principle of APs generated by neurons. This behavior can be expressed as

$$V_{mu} = \begin{cases} V_{\text{mu\_const}}, & V_{ep} \geq V_{mth} \\ 0, & V_{ep} < V_{mth}, \end{cases} \tag{10}$$

where $V_{\text{mu\_const}}$ is a constant waveform which is independent of stimulation strength. V_{mth} is the threshold for muscle fibers to generate APs. In the literature, its value is -50 mV [30].

AP transfers from postsynaptic membrane in NMJ to both sides along with the muscle fiber, which can be regarded as a current source. It can form a time-varying potential distribution on the skin surface. This is the principle of sEMG generation. Combining the spatial distribution of action potentials on muscle fibers, the action potential denoted as $V_{\text{mu\_const}}$ in (10) can be expressed as

$$V_m(z) = A(\lambda z)^3 e^{-\lambda z} - B, \tag{11}$$

where $A = 96$ mV is the amplitude of the action potential and $B = 90$ mV represents the resting membrane potential of the muscle fiber. These parameters are adopted in the reference paper [40]. λ is a scale factor expressed in mm^{-1}, its value can be selected as 1. z is the distance along the muscle fiber from NMJ to the recording site as shown in Fig. 4.

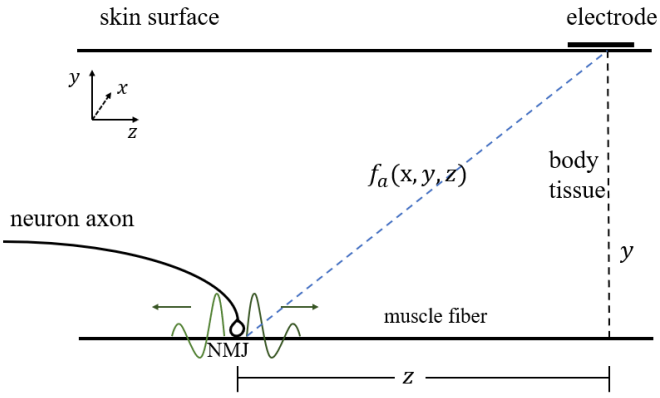

Fig. 4. Coordinate position representation of sEMG model [31]. The y-axis coordinate represents the depth of muscle fiber compared to the skin surface. The z-axis coordinate represents the horizontal distance from the external measuring electrode to the NMJ. $f_a(x, y, z)$ is the attenuation function of the SFAP.

The current distribution I_m is proportional to the second derivative of V_m, which can be expressed as

$$\begin{aligned} I_m(z) &= C\frac{d^2V_m(z)}{dz^2} \\ &= CA\lambda^2(\lambda z)[6 - 6\lambda z + (\lambda z)^2]e^{-\lambda z}. \end{aligned} \tag{12}$$

C is a proportionality constant which is formulated as

$$C = \frac{d_m^2 \sigma_a \pi}{4v^2}, \tag{13}$$

where d_m is the diameter of the muscle fiber. σ_a is the conductivity of the intracellular axoplasm. The conduction velocity of AP is denoted as v.

Reference [40] modeled the two action potentials which travels in opposite directions as two current tripoles. The propagation of the action potential from the muscle fiber to electrodes on the skin, is modeled as the propagation process of the current source in the volume conductor. In this paper, we use an attenuation function to represent the influence of human tissue during the transmission process [31]. This attenuation function is related to many factors, such as the distance between muscle fibers and electrodes, tissue conductivity and the radius of the muscle fiber. The expression is given as

$$f_a(x, y, z) = \frac{1}{4\pi\sigma_r} \frac{1}{\sqrt{z^2 + \frac{\sigma_z}{\sigma_r}[y^2 + x^2]}}, \tag{14}$$

where σ_r represents the radial conductivity of the external medium and σ_z is the axial extracellular conductivity. x, y, z is the coordinate of the electrode from the depolarization point of the muscle fiber. z is the distance along the fiber and y is the depth of the fiber from the skin surface.

In medicine, a motor neuron and its associated muscle fibers are called a motor unit (MU). The summation of the single-fiber action potentials (SFAPs) is called the motor unit action potential (MUAP). In general, we consider that the SFAPs in

the same MU fire simultaneously [41]. In practical applications, the recording of sEMG may contain multiple MUAPs. Fortunately, various techniques have been used to decompose composite sEMG signals. For our proposed framework, only one MUAP is used. The sEMG signal is formulated as

$$sEMG = K_m \cdot f_a(z) \cdot I_m(z) + n_s, \tag{15}$$

where K_m represents the number of muscle fibers contained in the MU and n_s is the noise. Considering that we only need to make a decision based on the sEMG signal in each time slot, so we only take the peak value of the sEMG signal in each time slot. If using bipolar surface electrodes, the sEMG signal can be described as

$$sEMG = sEMG(z_A) - sEMG(z_B), \tag{16}$$

where z_A and z_B are two different locations of the electrodes.

The sEMG signal is finally decoded at the external receiver. Since we use the OOK modulation scheme at the transmitter, we only need to determine whether the sEMG signal changes. When the sEMG signal changes greatly, for instance, greater than a threshold, it decodes to bit "1". The decoding strategy of the receiver is

$$\hat{x} = \begin{cases} \text{bit "1"}, & V_s \geq V_{th} \\ \text{bit "0"}, & V_s < V_{th}, \end{cases} \tag{17}$$

where V_{th} is the decision threshold and $\hat{x}$ is recovered information.

V. Feasibility Analysis

Usually, in the literature such as in the molecular communication field, it is assumed that the nanomachines in the IoNT can perform some tasks, such as encoding and decoding signals [36] [42]. These envisioned nanomachines can also perform some complex tasks by cooperation. However, it is right due to technical limitations, now we are still a few steps behind the Feynman-type nanorobots and performing intelligent and sophisticated functions need for further advances in many disciplines and research fields such as nanotechnology [43]. Of course, there is also some research work to provide ideas for the potential construction of these systems, such as synthetic biology based biological structures and nanomaterial-based methods [44].

For the base station in this paper, its implementation can also follow the same route as mentioned in [44]. For example, the base station must have both transmitting and receiving functions so that it can receive and then transmit the information from the nanomachines in IoNT to the neural channel. For the receiving function, the base station must contain three modules: the sensor module which is responsible for sensing signal molecules from other nanomachines; the transducer module which transforms the biological signals to some processable signals like electric signals; the processing module which decodes the received signals. For the transmitting function, this base station is similar to a traditional transmitter. It contains two main modules: the processing module which encodes information from IoNT as stimulus current; the stimulator module which implements the stimulation of the neuron.

There are many related studies in the literature for constructing these modules. For example, field effect transistor (FET)-based biosensors (bioFETs) can be used as the interface with the nanomachines in IoNT [44]–[46]. The bioFETs can realize electrical sensing which contain biosensors and transducers. We can use the biosensor based on natural receptor proteins, artificial single-stranded DNAs, and RNAs as the sensor module. And their sizes are small enough to be used in a nanomachine which is justified in the literature [44], [47], [48].

Then for the transmitting module in the base station, it can be implemented follows the way to design the implementable microstimulator as described in the literature [49]. Micro stimulators have attracted attention for a long time, and there are already quite a few applications of micro stimulators in medicine for the treatment of various diseases such as shoulder subluxation in poststroke pain, overactive bladder, and refractory headaches. Although there are still many challenges in the development of micro stimulators, it still has great potential. And the technical development and commercial interest may also accelerate its development.

Combining the micro stimulator with an electronic biosensor completes the main function of the base station. This is currently the most likely way to achieve it. From the aforementioned research of biosensors and microstimulators in the literature, it can be seen the possibility of constructing the BS in the paper. As long as the above technologies are mature enough, the current technical challenges may not be unsolvable in the future. It is also worth mentioning that the BS in this paper is not necessarily a nanomachine, because it performs the complex function of integrating information from IoNT and performing neuromodulation. It is difficult to accomplish by a single nanomachine.

VI. Mutual Information for Proposed System

The mutual information (MI) of two random variables X and Y is a measure of the inherent dependence between them. From the perspective of the whole communication system, mutual information represents the reduction of the uncertainty of the entire system after communication. Intuitively, it measures the information shared between X and Y. That is, when the value of one random variable is known, the amount by which the uncertainty of another random variable is reduced. If X represents the information sent by the transmitter and Y represents the information received by the receiver, the mutual information between X and Y is closely related to the statistical characteristics of the channel.

In information theory, the amount of information carried in the message depends on its surprising degree. The entropy is the measure of "surprise" inherent in the variable's possible outcomes. If an event is likely to happen, then it is not surprising when it happens as expected. Therefore, such messages carry almost no new information. The definition of mutual information is related to several information entropies. Specifically, marginal entropies $H(X)$ and $H(Y)$ represent priori uncertainty of X and Y. After communication, X

and Y establish a certain dependency through the channel. $H(X) - H(X|Y)$ represents the information shared by these two random variables, that is $I(X;Y)$. $H(X|Y)$ is the channel equivocation. It indicates the uncertainty that still exists for the random variable X after receiving the variable Y. It also represents the information lost in the channel. In this section, the mutual information of our proposed system is derived.

It can be seen from the action potential model in Section IV that the shape of the action potential at each node of Ranvier is the same. Axons can be regarded as highly reliable ideal channels. We presume the axon as an ideal channel without noise. Therefore, the input signal at the nerve fiber is also the input of the synaptic communication channel. In this paper, we ignore the neurotransmitter binding and releasing mechanism at the postsynaptic membrane and model the postsynaptic membrane as a perfectly absorbing receiver. Only a single nerve impulse denotes one transmitted symbol. When the symbol interval t_s is small, the previously transmitted symbols will cause inter-symbol interference. For example, there may be neurotransmitters released from previous time slots in the channel. Consider a symbol sequence $\{x_i, i = 1, 2, 3, \ldots\}$ from BS, where i denotes the number of time slot. Let Q_a^i denote the number of neurotransmitters absorbed in i^{th} time slot. Thus, Q_a^i can be expressed as

$$\begin{aligned} Q_a^i(t) =& Q_i + Q_{ISI} \\ =& Q x_i F(t_s) + \sum_{k=2}^{i} Q x_{i-k+1} \{F(kt_s) - F([k-1]t_s)\}. \end{aligned} \tag{18}$$

Q is the number of the released neurotransmitters for the symbol "1". $F(t)$ is hitting probability in (8), which expresses the fraction of signal molecules absorbed by receptors at the postsynaptic membrane. Hitting probability is actually the time integral of the hitting rate which is the channel impulse response (CIR) for the synaptic MC channel. The expressions are

$$\begin{aligned} F(t_s) &= \int_0^{t_s} f_{hit}(x)dx, \\ f_{hit}(t) &= \frac{r}{d+r} \frac{1}{\sqrt{4\pi D t}} \frac{d}{t} \cdot e^{-\frac{d^2}{4Dt}}, \end{aligned} \tag{19}$$

where $f_{hit}(t)$ denotes the hitting rate of neurotransmitters. Other parameters have the same meaning as in (8).

$Q_a(t)$ contains the neurotransmitters released at current time interval Q_i for symbol x_i and the remainder neurotransmitters Q_{ISI} of the previous symbols. This number of molecules bound with the receiver follows Gaussian distribution [50]. Thus,

$$Q_a^i \sim N(\mu^i, [\sigma^2]^i). \tag{20}$$

The expectation and variance of this Gaussian distribution are

$$\begin{aligned} \mu^i =& Q \sum_{k=1}^{i} p_k x_{i-k+1}, \\ [\sigma^2]^i =& Q \sum_{k=1}^{i} p_k (1-p_k) x_{i-k+1}, \end{aligned} \tag{21}$$

where Q is the number of neurotransmitters released into the cleft for the bit "1" in one time slot. Here we take the expectation value $p_r N_n n_v$ in (7). p_k is the hitting probabilities of neurotransmitters in k^{th} time slot from the time when the neurotransmitter is released. p_k can be calculated as follows [39]

$$p_k = \begin{cases} F(t_s), & k = 1 \\ F(kt_s) - F([k-1]t_s), & k > 1, \end{cases} \tag{22}$$

where t_s denotes the duration of the time slot. Because the transmitter and receiver are static in synaptic communication, $(\mu^i, [\sigma^2]^i)$ in each time slot remains the same.

We assume that ISI mitigation technique is used to mitigate its impact on the number of neurotransmitters received at the receiver [51]. Therefore, the expected number for bit "1" and bit "0", denoted as μ_1 and μ_0 respectively, can be expressed as

$$\begin{aligned} \mu_1 =& QF(t_s), \\ \mu_0 =& 0. \end{aligned} \tag{23}$$

It is noticed that the distribution of received signal molecules at the receiver for bit "0" obeys the Gaussian distribution with a mean value of 0. From a practical point of view, it is impossible for the receiver to receive a negative number of signal molecules. We can avoid this problem by changing the modulation method at the transmitter. However, in the previous section of this paper, we have selected the OOK modulation method. So we temporarily ignore this problem and still use this Gaussian distribution to calculate its mutual information during the simulation.

The influence of ISI on the variance of the number of neurotransmitters received cannot be eliminated [52]. Assuming the probabilities of BS sending bit "1" and bit "0" are p^1 and p^0 respectively. Thus, variance for bit "1" and bit "0", denoted as σ_1^2 and σ_0^2 respectively, can be expressed as

$$\begin{aligned} \sigma_1^2 =& QF(t_s)(1 - F(t_s)) + p^1 Q \sum_{k=2}^{i} p_k (1-p_k), \\ \sigma_0^2 =& p^1 Q \sum_{k=2}^{i} p_k (1-p_k). \end{aligned} \tag{24}$$

In Section IV, we introduced that the release of vesicles is random. We regard this randomness as noise of the channel with zero mean and variance expressed as

$$\sigma_c^2 = p_r(1-p_r) N_n n_v. \tag{25}$$

Then the probability model of the number of neurotransmitters received by postsynaptic membrane updates to the superimposed distribution of two independent Gaussian distributions. The expectations remain the same for the two symbols and the two variances are updated to

$$\begin{aligned} \sigma_1^2 =& QF(t_s)(1 - F(t_s)) + p^1 Q \sum_{k=2}^{i} p_k (1-p_k) + \sigma_c^2, \\ \sigma_0^2 =& p^1 Q \sum_{k=2}^{i} p_k (1-p_k) + \sigma_c^2. \end{aligned} \tag{26}$$

With these parameters we can get the probability density function (PDF) of received neurotransmitters in the i^{th} time interval for these two symbols.

In (9) the relationship between endplate membrane potential and the number of neurotransmitters are defined as linear. From Section IV, it is known that when the position of electrodes is fixed on the skin surface, the relationship between sEMG and $V_m(z)$ can be seen as determinate without considering the unsystematic error. Thus, we detect signal by comparing the number of received neurotransmitters, denoted as y_i, to a threshold, denoted as y_{th}. The detected symbol at the receiving end of the system can be expressed as

$$\hat{y} = \begin{cases} \text{bit “1”}, & y_i \geq y_{th} \\ \text{bit “0”}, & y_i < y_{th}, \end{cases} \tag{27}$$

The error probabilities of each symbol are [52]

$$\begin{aligned} P_{xy}(1|0) &= \int_{y_{th}}^{+\infty} \frac{1}{\sqrt{2\pi}\sigma_0} exp[\frac{-(y_i-\mu_0)^2}{2\sigma_0^2}]dy \\ &= fQ(\frac{y_{th}-\mu_0}{\sigma_0}), \\ P_{xy}(0|1) &= \int_{-\infty}^{y_{th}} \frac{1}{\sqrt{2\pi}\sigma_1} exp[\frac{-(y_i-\mu_1)^2}{2\sigma_1^2}]dy \\ &= 1 - fQ(\frac{y_{th}-\mu_1}{\sigma_1}), \end{aligned} \tag{28}$$

where $fQ(\cdot)$ is the Q function. The bit error probability for the synaptic channel, denoted as P_e, then can be presented as

$$P_e = p^1 P_{xy}(0|1) + p^0 P_{xy}(1|0). \tag{29}$$

In order to calculate mutual information we need the joint probabilities which are derived as

$$\begin{aligned} p(0,0) &= p^0(1 - P_{xy}(1|0)), \\ p(0,1) &= p^0 P_{xy}(1|0), \\ p(1,0) &= p^1 P_{xy}(0|1)), \\ p(1,1) &= p^1(1 - P_{xy}(0|1)). \end{aligned} \tag{30}$$

In addition, the marginal probabilities are needed

$$\begin{aligned} p(x) &= p(x,0) + p(x,1), \\ p(y) &= p(0,y) + p(1,y). \end{aligned} \tag{31}$$

Then, we can calculate the mutual information by

$$I(X;Y) = \sum_{y\in Y}\sum_{x\in X} p(x,y)\log\frac{p(x,y)}{p(x)p(y)}. \tag{32}$$

Here, X denotes the random variable at the transmitter, and Y denotes the random variable at the receiving end of the system.

VII. Numerical Results

In this section, the error probability and mutual information of this interface system is evaluated by MATLAB. The relationship between error probability and some important parameters, such as diffusion coefficient, synapse membrane distance and decision threshold, are investigated. The impact of these parameters on the mutual information is also presented. Simulation parameters are shown in Table II.

TABLE II
Simulation Parameters

Parameter	Value
Diffusion coefficient D	4×10^{-12}–2.5×10^{-10} (m^2/s) [53]
Synapse membrane distance d	10–60 (nm) [54]
Symbol interval t_s	0.2–1.8 (ms) [37]
Released neurotransmitters Q	9500-20000 [37] [55]
Decision threshold	0–600
Symbol probability of bit “1” p_0	0.1–0.9

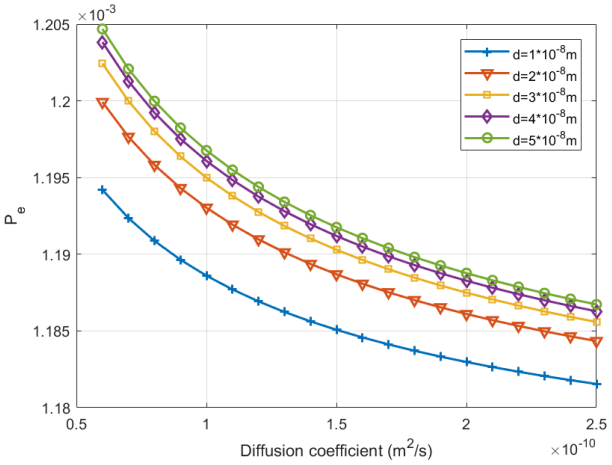

Fig. 5. The relationship between diffusion coefficient and error probability when the distances of the synaptic cleft are different.

The relationship of distance, diffusion coefficient, and error probability P_e is shown in Fig. 5. Here we define Q in (5) as 10000 when an AP is transmitted to the synapse. We choose symbol intervals equal to 1 ms. From (9) and (10), it can be seen that the number of neurotransmitters bound to receptors is directly related to whether the postsynaptic muscle fiber is activated. Define the threshold as $Q_a = 200$. The distances between synapse membranes are from 10 nm to 50 nm. Considering that there may be neurotransmitters from the last AP transmission but not cleared in time in the synaptic cleft, the inter-symbol interference influence is considered. Assume that ISI effect lasts for four bit intervals which is 1 ms for each one. Moreover, the probabilities of sending bit “1” and bit “0” are all 0.5 at the BS. The receiving radius r is 6 nm.

From Fig. 5, we know that P_e decreases as D increases. It is because the increase of D leads to the decrease of $\frac{d}{\sqrt{4Dt}}$. $erfc(\cdot)$ is a monotonically decreasing function, thus, $F(t)$ will increase as the increase of D. Then more neurotransmitters will reach the postsynaptic membrane, producing a further larger V_{ep}. A larger V_{ep} is more likely to trigger muscle fiber AP, which will eventually generate sEMG and allow the receiver to detect the transmitted signal.

It is also obvious that as d increases, P_e increases. This is because the increase of d leads to the decrease of $F(t)$. Fewer neurotransmitters arrive at postsynaptic membrane which leads

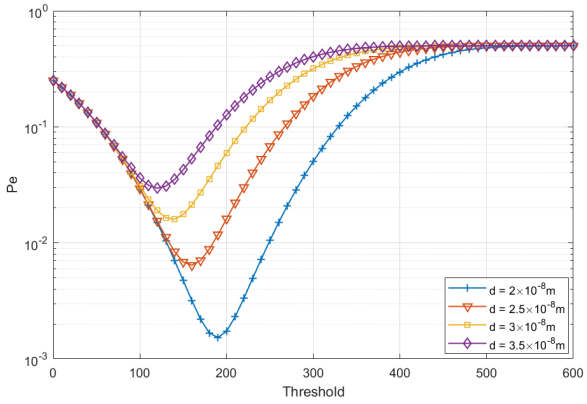

Fig. 6. The relationship of the error probability and decision threshold at the receiver for different synapse membrane distances.

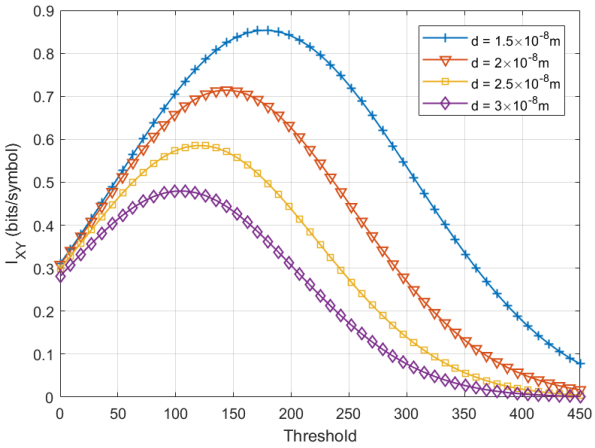

Fig. 7. The relationship of the mutual information and decision threshold at the receiver for different synapse membrane distances.

to smaller V_{ep}. So it is more difficult to cause muscle fibers to generate APs, which ultimately makes the receiver relatively unlikely to detect the transmitted signal.

In Fig. 6, the impact of threshold and distance between the presynaptic membrane and the postsynaptic membrane on the error performance is presented. According to the synaptic physiological data, we set the distance between synapse membranes from 20 nm to 50 nm [54]. It is defined that Q in (5) is 20000 when an AP travels on the axon. The diffusion coefficient is set as 6×10^{-11} m^2/s [53]. It can be seen from curves that the choice of the threshold has a great impact on the performance of the system. When the other parameters are stable, there is an optimal decision threshold to make the system error probability the lowest. However, the distance between the membranes determines the lowest possible level of system error probability. Mutual information with respect to the threshold is also investigated which is shown in Fig. 7. It shows the opposite trend to the error probability curve. When the appropriate threshold is selected, the error probability decreases whereas the mutual information increases with respect to the decrease of membrane distance.

Fig. 8 and Fig. 9 show the impact of diffusion coefficient, synapse distance and symbol interval on the mutual information. When diffusion coefficient increases, mutual information shows a rising trend. The reason is similar to the reason for the decrease of error probability mentioned in Fig. 5. In Fig. 9, it is noticed that the MI increases with increasing symbol interval. The reason can be inferred from (18) and (19). In the presence of ISI, increasing the symbol interval can reduce ISI, thereby increasing the amount of information transmitted and increasing mutual information.

In Fig. 10 and Fig. 11, the impact of symbol probability, distance of synapse membranes, and the number of molecules released on the mutual information is investigated. It is obvious in Fig. 10 that the mutual information increases as the distance decreases. In addition, it can be seen from Fig. 11 that when the number of neurotransmitters released by the nerve terminal increases, the error probability decreases and the mutual information increases. It is also noticed that the mutual information

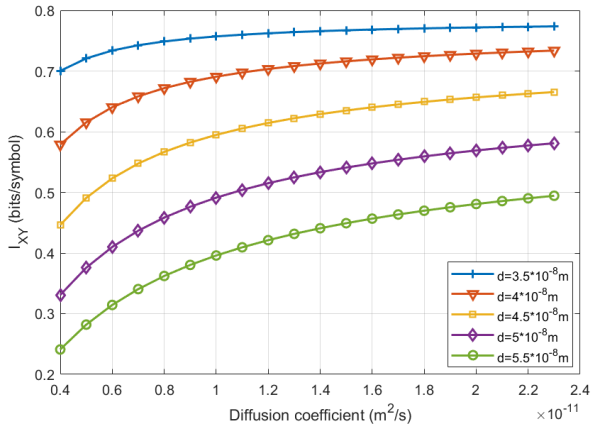

Fig. 8. The relationship of the mutual information and diffusion coefficient for different synapse membrane distances.

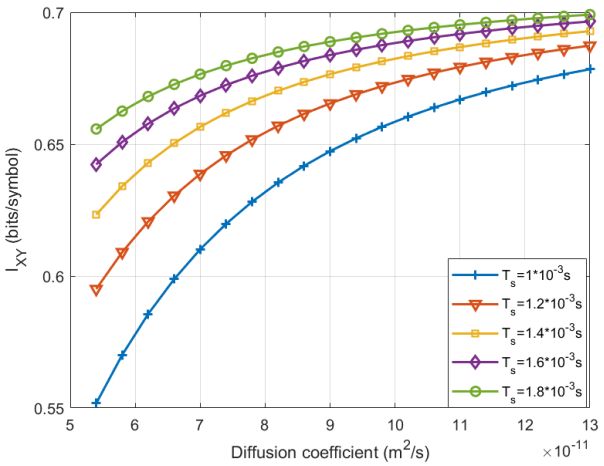

Fig. 9. The relationship of the mutual information and diffusion coefficient for different symbol intervals.

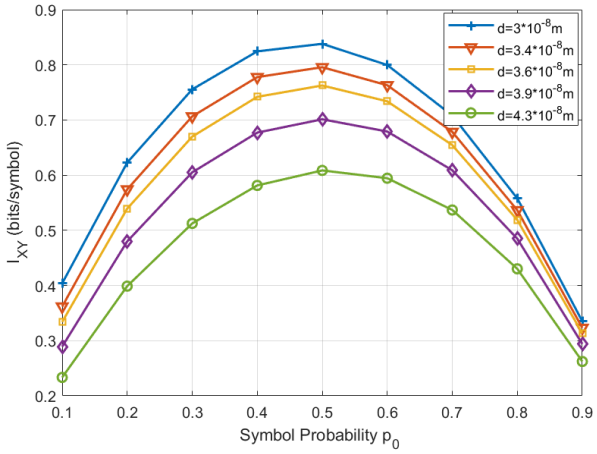

Fig. 10. The relationship of the mutual information and symbol probability for different synapse membrane distances.

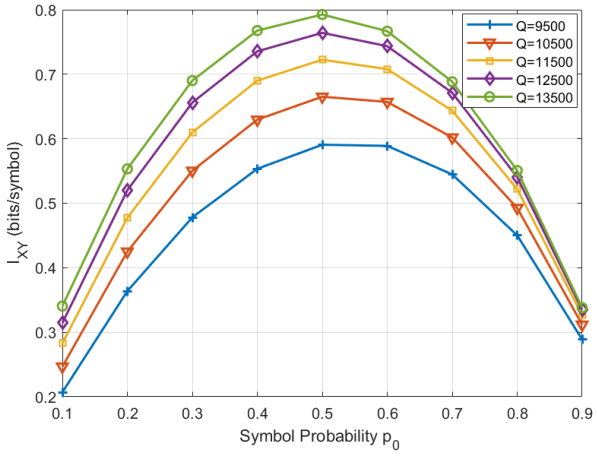

Fig. 11. The relationship of the mutual information and symbol probability for different number of neurotransmitters released for one nerve impulse.

curve is not symmetric about $p_0 = 0.5$. For example, for the first three curves on Fig. 10, I_{XY} at $p_0 = 0.1$ is larger than that at $p_0 = 0.9$. However, for the two curves below in Fig. 10, the mutual information at $p_0 = 0.1$ is smaller than that at $p_0 = 0.9$. This is because for the different distances, the optimal thresholds are different. In this simulation we set the threshold fixed as $Q_a = 130$. As the distance increases, μ_1 at the receiver decreases. Therefore, the selected threshold gradually approaches μ_1, so that $P_{xy}(1|0) > P_{xy}(0|1)$ becomes $P_{xy}(1|0) < P_{xy}(0|1)$. Hence, for the first three curves if $p_0 = 0.9$, more bit "0" are transmitted, the error probability increases and mutual information decreases than $p_0 = 0.1$.

The impact of ISI on mutual information is shown in Fig. 12. It can be seen from the figure that the larger the length of the ISI, the smaller the mutual information obtained. The reason is obvious. The increase in ISI can increase the value of σ_1^2 and σ_0^2 in (26), thereby increasing the error probability and reducing the mutual information.

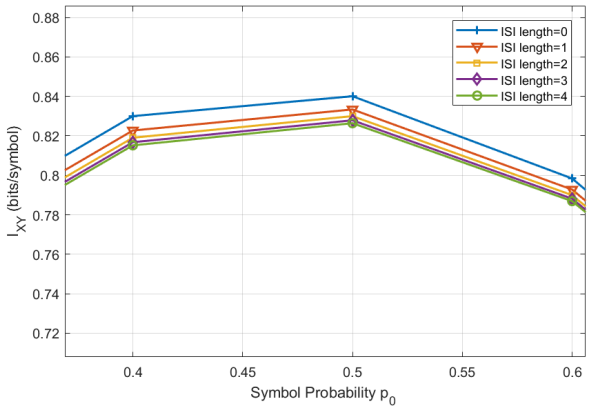

Fig. 12. The relationship of the mutual information and symbol probability with different ISI length.

VIII. Conclusion

In this paper, we propose a novel through-body communication system which is used as an interface between in-vivo IoNT and external devices. Inspired by neural communication and the way organisms interact with the environment, we propose that the neural pathway can be used to transfer signals sent by MC nodes to extracorporeal networks through electric stimulation. The framework of the entire interface system and corresponding mathematical model are introduced. Mutual information of this system is derived in the paper. The error performance and mutual information are evaluated. This study will pave the way for the connection of IoNTs in vivo to external networks. Future work would focus on experiments on living animal bodies.

References

[1] Y. Li, L. Lin, W. Guo, and H. Yan, "Signal transmission through human body via engineered nervous system," in *Proc. IEEE Global Commun. Conf. (GLOBECOM)*. IEEE, Dec, 2020.

[2] T. Luo, R. Zheng, J. Song, L. Lin, and H. Yan, "A small-scale modulator of electric-to-biological signal conversion for synthetic molecular communications," in *Proc. IEEE ICC*. IEEE, 2020, pp. 1–7.

[3] I. F. Akyildiz, F. Brunetti, and C. Blázquez, "Nanonetworks: A new communication paradigm," *Comput. Netw.*, vol. 52, no. 12, pp. 2260–2279, 2008.

[4] L. Lin, F. Huang, H. Yan, F. Liu, and W. Guo, "Ant-behavior inspired intelligent nanonet for targeted drug delivery in cancer therapy," *IEEE Trans. NanoBiosci.*, vol. 19, no. 3, pp. 323–332, 2020.

[5] T. Nakano, "Molecular communication: A 10 year retrospective," *IEEE Trans. Mol. Biol. Multi-Scale Commun.*, vol. 3, no. 2, pp. 71–78, 2017.

[6] D. Malak and O. B. Akan, "Molecular communication nanonetworks inside human body," *Nano Commun. Netw.*, vol. 3, no. 1, pp. 19–35, 2012.

[7] I. F. Akyildiz, M. Pierobon, S. Balasubramaniam, and Y. Koucheryavy, "The internet of bio-nano things," *IEEE Commun. Mag.*, vol. 53, no. 3, pp. 32–40, 2015.

[8] B. Atakan, O. B. Akan, and S. Balasubramaniam, "Body area nanonetworks with molecular communications in nanomedicine," *IEEE Commun. Mag.*, vol. 50, no. 1, pp. 28–34, 2012.

[9] E. Omanović-Mikličanin, M. Maksimović, and V. Vujović, "The future of healthcare: nanomedicine and internet of nano things," *Folia Medica Fac. Medicinae Univ. Saraeviensis*, vol. 50, no. 1, pp. 23–28, 2015.

[10] L. Felicetti, M. Femminella, G. Reali, and P. Liò, "A molecular communication system in blood vessels for tumor detection," in *Proc. ACM 1st Annu. Int. Conf. Nanosc. Comput. Commun.*, 2014, pp. 1–9.

[11] T. Nakano, S. Kobayashi, T. Suda, Y. Okaie, Y. Hiraoka, and T. Haraguchi, "Externally controllable molecular communication," *IEEE J. Sel. Areas Commun.*, vol. 32, no. 12, pp. 2417–2431, 2014.

[12] S. Kisseleff, R. Schober, and W. H. Gerstacker, "Magnetic nanoparticle based interface for molecular communication systems," *IEEE Commun. Lett.*, vol. 21, no. 2, pp. 258–261, 2016.

[13] J. Heikenfeld, "Let them see you sweat," *IEEE Spectr.*, vol. 51, no. 11, pp. 46–63, 2014.

[14] A. Einolghozati, M. Sardari, and F. Fekri, "Design and analysis of wireless communication systems using diffusion-based molecular communication among bacteria," *IEEE Trans. Wireless Commun.*, vol. 12, no. 12, pp. 6096–6105, 2013.

[15] G. J. Tortora and B. H. Derrickson, *Principles of anatomy and physiology*. John Wiley & Sons, 2018.

[16] D. Malak and O. B. Akan, "Communication theoretical understanding of intra-body nervous nanonetworks," *IEEE Commun. Mag.*, vol. 52, no. 4, pp. 129–135, 2014.

[17] M. T. Barros, "Capacity of the hierarchical multi-layered cortical microcircuit communication channel," in *Proc. ACM 5th Annu. Int. Conf. Nanosc. Comput. Commun.*, 2018, pp. 1–6.

[18] O. B. Akan, H. Ramezani, M. Civas, O. Cetinkaya, B. A. Bilgin, and N. A. Abbasi, "Information and communication theoretical understanding and treatment of spinal cord injuries: State-of-the-art and research challenges," *IEEE Rev. Biomed. Eng.*, 2021.

[19] N. A. Abbasi, D. Lafci, and O. B. Akan, "Controlled information transfer through an in vivo nervous system," *Sci. Rep.*, vol. 8, no. 1, pp. 1–12, 2018.

[20] W. Schuepbach, J. Rau, K. Knudsen, J. Volkmann, P. Krack, L. Timmermann, T. Hälbig, H. Hesekamp, S. Navarro, N. Meier *et al.*, "Neurostimulation for parkinson's disease with early motor complications," *N. Engl. J. Med.*, vol. 368, no. 7, pp. 610–622, 2013.

[21] C. Koca, E. Dinc, H. Ramezani, and O. Akan, "Performance analysis for capacitive electrical neural interfaces," in *Proc. IEEE 18th Int. Conf. Nanotechnol. (IEEE-NANO)*. IEEE, 2018, pp. 1–4.

[22] "Action potential — Wikipedia, the free encyclopedia," https://en.wikipedia.org/w/index.php?title=Action_potential&oldid=958647466, 2020, [Online; accessed 26-May-2020].

[23] J. W. Kalat, *Biological psychology*. Nelson Education, 2015.

[24] R. Lewis, K. E. Asplin, G. Bruce, C. Dart, A. Mobasheri, and R. Barrett-Jolley, "The role of the membrane potential in chondrocyte volume regulation," *J. Cell. Physiol.*, vol. 226, no. 11, pp. 2979–2986, 2011.

[25] M. A. Eckert, P. Q. Vu, K. Zhang, D. Kang, M. M. Ali, C. Xu, and W. Zhao, "Novel molecular and nanosensors for in vivo sensing," *Theranostics*, vol. 3, no. 8, p. 583, 2013.

[26] L. R. Sheffler and J. Chae, "Neuromuscular electrical stimulation in neurorehabilitation," *Muscle & Nerve*, vol. 35, no. 5, pp. 562–590, 2007.

[27] E. R. Kandel, J. H. Schwartz, T. M. Jessell, D. of Biochemistry, M. B. T. Jessell, S. Siegelbaum, and A. Hudspeth, *Principles of neural science*. McGraw-hill New York, 2000, vol. 4.

[28] D. R. McNeal, "Analysis of a model for excitation of myelinated nerve," *IEEE Trans. Biomed. Eng.*, no. 4, pp. 329–337, 1976.

[29] X. Zhang, J. R. Roppolo, W. C. De Groat, and C. Tai, "Mechanism of nerve conduction block induced by high-frequency biphasic electrical currents," *IEEE Trans. Biomed. Eng.*, vol. 53, no. 12, pp. 2445–2454, 2006.

[30] S. J. Wood and C. R. Slater, "Safety factor at the neuromuscular junction," *Prog. Neurobiol.*, vol. 64, no. 4, pp. 393–429, 2001.

[31] K. A. Wheeler, D. K. Kumar, and H. Shimada, "An accurate bicep muscle model with semg and muscle force outputs," *J. Med. Biol. Eng.*, vol. 30, no. 6, pp. 393–398, 2010.

[32] M. M. Lowery, C. L. Vaughan, P. J. Nolan, and M. J. O'Malley, "Spectral compression of the electromyographic signal due to decreasing muscle fiber conduction velocity," *IEEE Trans. Rehabilitation Eng.*, vol. 8, no. 3, pp. 353–361, 2000.

[37] T. Khan, B. A. Bilgin, and O. B. Akan, "Diffusion-based model for synaptic molecular communication channel," *IEEE Trans. Nanobiosci.*, vol. 16, no. 4, pp. 299–308, 2017.

[33] R. Nayak and R. K. Banik, "Current innovations in peripheral nerve stimulation," *Pain Res. Treat.*, vol. 2018, 2018.

[34] B. Katz, "Quantal mechanism of neural transmitter release," *Science*, vol. 173, no. 3992, pp. 123–126, 1971.

[35] R. H. Edwards, "The neurotransmitter cycle and quantal size," *Neuron*, vol. 55, no. 6, pp. 835–858, 2007.

[36] N. Farsad, H. B. Yilmaz, A. Eckford, C.-B. Chae, and W. Guo, "A comprehensive survey of recent advancements in molecular communication," *IEEE Commun. Surveys Tuts.*, vol. 18, no. 3, pp. 1887–1919, 2016.

[38] S. Lotter, A. Ahmadzadeh, and R. Schober, "Channel modeling for synaptic molecular communication with re-uptake and reversible receptor binding," in *Proc. IEEE ICC*. IEEE, 2020, pp. 1–7.

[39] B. Tepekule, A. E. Pusane, H. B. Yilmaz, C.-B. Chae, and T. Tugcu, "ISI mitigation techniques in molecular communication," *IEEE Trans. Mol. Biol. Multi-Scale Commun.*, vol. 1, no. 2, pp. 202–216, 2015.

[40] R. Merletti, L. L. Conte, E. Avignone, and P. Guglielminotti, "Modeling of surface myoelectric signals. i. model implementation," *IEEE Trans. Biomed. Eng.*, vol. 46, no. 7, pp. 810–820, 1999.

[41] J. S. Karlsson, K. Roeleveld, C. Grönlund, A. Holtermann, and N. Östlund, "Signal processing of the surface electromyogram to gain insight into neuromuscular physiology," *Philos. Trans. Royal Soc. A*, vol. 367, no. 1887, pp. 337–356, 2009.

[42] L. Felicetti, M. Femminella, G. Reali, and P. Liò, "Applications of molecular communications to medicine: A survey," *Nano Commun. Netw.*, vol. 7, pp. 27–45, 2016.

[43] E. Ellis, S. Moorthy, W.-I. K. Chio, and T.-C. Lee, "Artificial molecular and nanostructures for advanced nanomachinery," *Chem. Comm.*, vol. 54, no. 33, pp. 4075–4090, 2018.

[44] M. Kuscu, E. Dinc, B. A. Bilgin, H. Ramezani, and O. B. Akan, "Transmitter and receiver architectures for molecular communications: A survey on physical design with modulation, coding, and detection techniques," *Proceedings of the IEEE*, vol. 107, no. 7, pp. 1302–1341, 2019.

[45] S. Xu, J. Zhan, B. Man, S. Jiang, W. Yue, S. Gao, C. Guo, H. Liu, Z. Li, J. Wang *et al.*, "Real-time reliable determination of binding kinetics of dna hybridization using a multi-channel graphene biosensor," *Nat. Commun.*, vol. 8, no. 1, pp. 1–10, 2017.

[46] J. Shan, J. Li, X. Chu, M. Xu, F. Jin, X. Wang, L. Ma, X. Fang, Z. Wei, and X. Wang, "High sensitivity glucose detection at extremely low concentrations using a mos 2-based field-effect transistor," *RSC advances*, vol. 8, no. 15, pp. 7942–7948, 2018.

[47] K. R. Rogers, "Principles of affinity-based biosensors," *Mol. Biotechnol.*, vol. 14, no. 2, pp. 109–129, 2000.

[48] A. Poghossian and M. J. Schöning, "Label-free sensing of biomolecules with field-effect devices for clinical applications," *Electroanalysis*, vol. 26, no. 6, pp. 1197–1213, 2014.

[49] B. Pless and A. M. Goodman, "Microstimulators: Minimally invasive implantable neuromodulatory devices," in *Neuromodulation*. Elsevier, 2018, pp. 289–303.

[50] T. Nakano, A. W. Eckford, and T. Haraguchi, *Molecular communication*. Cambridge University Press, 2013.

[51] G. Chang, L. Lin, and H. Yan, "Adaptive detection and ISI mitigation for mobile molecular communication," *IEEE Trans. Nanobiosci.*, vol. 17, no. 1, pp. 21–35, 2017.

[52] L. Lin, Q. Wu, F. Liu, and H. Yan, "Mutual information and maximum achievable rate for mobile molecular communication systems," *IEEE Trans. NanoBiosci.*, vol. 17, no. 4, pp. 507–517, 2018.

[53] L. Lin, J. Zhang, M. Ma, and H. Yan, "Time synchronization for molecular communication with drift," *IEEE Commun. Lett.*, vol. 21, no. 3, pp. 476–479, 2016.

[54] F. Gabbiani and S. J. Cox, *Mathematics for neuroscientists*. Academic Press, 2017.

[55] T. Khan, H. Ramezani, G. Muzio, and O. Akan, "Analysis of information flow in miso neuro-spike communication channel with synaptic plasticity," in *Proc. IEEE 18th Int. Conf. Nanotechnol. (IEEE-NANO)*. IEEE, 2018, pp. 1–4.

Error performance and mutual information for IoNT interface system

Li, Yu

2022-02-23

Li Y, Lin L, Guo W, et al., (2022) Error performance and mutual information for IoNT interface system. IEEE Internet of Things Journal, Volume 9, Number 12, 15 June 2022, pp. 9831-9842
https://doi.org/10.1109/JIOT.2022.3153637